Nuclear Astrophysics at n_TOF, CERN

G Tagliente[1], U Abbondanno[2], G Aerts[3], H Alvarez[4], F Alvarez-Velarde[5], S Andriamonje[3], J Andrzejewski[6], L Audouin[8], G Badurek[9], P Baumann[10], F Bečvář[11], F Belloni[2], E Berthoumieux[3], S Bisterzo[12], F Calviño[13], M Calviani[14], D Cano-Ott[5], R Capote[15,16], C Carrapiço[17], P Cennini[18], V Chepel[19], E Chiaveri[18], N Colonna[1], G Cortes[13], A Couture[20], J Cox[20], M Dahlfors[18], S David[10], I Dillman[8], C Domingo-Pardo[21], W Dridi[3], I Duran[4], C Eleftheriadis[22], M Embid-Segura[5], A Ferrari[18], R Ferreira-Marques[19], K Fujii[2], W Furman[24], R Gallino[12], I Goncalves[19], E Gonzalez-Romero[5], F Gramegna[14], C Guerrero[5], F Gunsing[3], B Haas[25], R Haight[26], M Heil[8], A Herrera-Martinez[18], M Igashira[27], E Jericha[9], F Käppeler[8], Y Kadi[18], D Karadimos[7], D Karamanis[7], M Kerveno[10], P Koehler[28], E Kossionides[29], M Krtička[11], H Leeb[9], A Lindote[19], I Lopes[19], M Lozano[16], S Lukic[10], J Marganiec[6], S Marrone[1], T Martinez[5], C Massimi[30], P Mastinu[14], A Mengoni[15], P M Milazzo[2], M Mosconi[8], F Neves[19], H Oberhummer[9], J Pancin[3], C Papachristodoulou[7], C Papadopoulos[31], C Paradela[4], N Patronis[7], A Pavlik[32], P Pavlopoulos[33], L Perrot[3], M T Pigni[9], R Plag[8], A Plompen[34], A Plukis[3], A Poch[13], J Praena[14], C Pretel[13], J Quesada[16], T Rauscher[35], R Reifarth[26], C Rubbia[36], G Rudolf[10], P Rullhusen[34], J Salgado[17], C Santos[17], L Sarchiapone[18], I Savvidis[22], C Stephan[23], J L Tain[21], L Tassan-Got[23], L Tavora[17], R Terlizzi[1], G Vannini[30], P Vaz[17], A Ventura[37], D Villamarin[5], M C Vincente[5], V Vlachoudis[18], R Vlastou[31], F Voss[8], S Walter[8], H Wendler[18], M Wiescher[20] and K Wisshak[8]

[1] INFN, Bari, Italy; [2]INFN, Trieste, Italy; [3]CEA/Irfu, Gif-sur-Yvette, France; [4]Univ. Santiago de Compostela, Spain; [5]CIEMAT, Madrid, Spain; [6]Univ. Lodz, Poland; [7]Univ. Ioannina, Greece; [8]FZK, Institut fűr Kernphysik, Germany; [9]Technische Universität Wien, Austria; [10]CNRS/IN2P3 - IReS, Strasbourg, France; [11]Univ. Prague, Czech Republic; [12]Dip. Fisica Generale, Univ. Torino, Italy; [13]Univ. Politecnica Catalunya, Barcelona, Spain; [14]INFN, Laboratori Nazionali di Legnaro, Italy; [15]IAEA, Vienna, Austria; [16]Univ. Sevilla, Spain; [17]ITN, Lisbon, Portugal; [18]CERN, Geneva, Switzerland; [19] LIP - Coimbra & Dep. Fisica Univ. Coimbra, Portugal; [20]Univ. Notre Dame, USA; [21]Inst. Fisica Corpuscular, CSIC-Univ. Valencia, Spain; [22]Aristotle Univ. Thessaloniki, Greece; [23]CNR S/IN2P3 - IPN, Orsay, France; [24]JINR, Frank Lab. Neutron Physics, Dubna, Russia; [25]CNRS/IN2P3 - IPN, Orsay, France; [26]LANL, USA; [27]Tokyo Inst. Technology, Japan; [28]ORNL, Physics Division, USA; [29]NCSR, Athens, Greece; [30]Dip. Fisica, Univ. Bologna, & INFN, Bologna, Italy; [31]National Technical Univ. Athens, Greece; [32]Inst. fűr Fakultät fűr Physik, Univ. Wien, Austria; [33]Pôle Univ. L. de Vinci, Paris, France; [34]CEC-JRC-IRMM, Geel, Belgium; [35]Dep. Physics and Astronomy, Univ. Basel, Switzerland; [36]Univ. Pavia,Italy; [37]ENEA, Bologna, Italy. The n_TOF Collaboration

Abstract

The neutron time of flight (n_TOF) facility at CERN is a spallation neutron source with white neutron energy spectrum (from thermal to several GeV), covering the full energy range of interest for nuclear astrophysics, in particular for measurements of the neutron capture cross section required in s-process nucleosynthesis. This contribution presents an overview on the astrophysical program carried on at the n_TOF facility, the main results and their implications.

1 Stellar nucleosyntesis

The origin of the elements is an important topic to understand the evolution of the universe. Hydrogen and helium, and small amounts of lithium, were formed in the period between about 100 seconds and 20 minutes after the big bang [1]. This period of primordial nucleosynthesis was followed by galactic condensation and the formations of the stars. All elements heavier than lithium have been formed in stars, and the elements heavier than iron have been formed via neutron capture processes in the stars. The isotopic abundances in the solar system reflect the average composition of the galaxy as it was 5.5 x 10^9 years ago. Spectral information of stellar environments and isotopic analyses of presolar dust grains provide important observation to validate stellar evolution models.

1.1 The s-process

Stellar nucleosynthesis has first been extensively reviewed in the reference work [2] and more recently in [3][4]. The isotopes up to ^{56}Fe can be synthesized by fusion reactions during the different stages of the evolution of a star. It is nowadays well established that neutron capture processes in red giant stars and supernovae are responsible for the formation of nearly all isotopes with higher masses [1][5]. This was first recognized by the discovery of technetium in red giant [6].

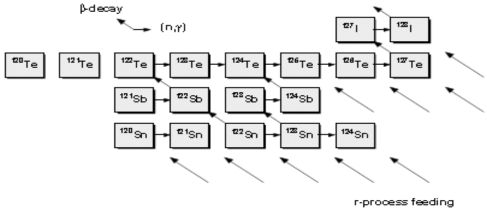

Fig.1 s-process path in the Sn region with s-only and r-only isotopes

The neutron capture mechanisms are known as s- and r-processes, where “s” stands for slow and “r” for rapid referring to the time scale of the β-decay. The s- and r- processes are important for the stable and neutron rich isotopes. A thorough knowledge of the s-process, for which much more experimental data is available, constrains the possibilities of the r-process. A competing mechanism is the p-process, referring to photodisintegration reaction like (γ,n), (γ,p) and (γ,α), they influence the abundances from the proton rich side.

isotopes from ^{56}Fe to ^{209}Bi are formed. Heavier nuclei than Bi are unstable and cannot be formed by neutron capture anymore. The s-process path follows closely the valley of stability in the chart of the nuclei and ends at ^{209}Bi. The neutron source of the s-process are manly the ^{22}Ne(α,n)^{25}Mg and ^{13}C(α,n)^{16}O reactions

In the r-process the neutron capture process is much faster and occurs on much shorter time scales. The time between consecutive neutron captures is of the order of seconds. To achieve the according extremely high neutron fluxes, the astrophysical site for the r-process is believed to be of explosive nature, like in a supernova or in merging neutron stars.

Neutron capture cross section are a key ingredient in the development of stellar models using the calculation of nuclear abundances in stellar environments. At the branching points uncertainties in the cross sections can propagate into large differences in the production of higher mass nuclei within a given model.

In a very schematic quantitative description of the s-process, starting from the seed nucleus ^{56}Fe and assuming constant temperature and neutron density, for a s-only nucleus the product of the average capture cross section $\langle\sigma_\gamma\rangle_{kT,A}$ and the abundance of the isotope $N_{s,A}$ constant

$$\langle\sigma_\gamma\rangle_{\mathbf{kT,A}}\,\mathbf{N_{s,A} = constant} \qquad (1)$$

Indeed this is roughly the case, except for the nuclei with magic numbers (N = 28,50,82,126) around A = 88, 140, and 208, which have very low cross sections. These nuclei are bottlenecks in the s-process paths, and show up as abundance peaks. The s-only nuclei are shielded from r-process by stable isobars of nuclei with lower Z and which contributions from proton rich side of the valley of stability are commonly neglected. In the same way r-only nuclei have no contribution from the s-process.

In fig 1 a simplified part of the s-process is shown in the Z = 50 vicinity starting from ^{120}Sn. Some stable nuclides, like ^{124}Sn and ^{130}Te are not reached by the s-process put but are shielded from r-process by the nuclei ^{122}Sb, ^{123}Sb and ^{124}Sb. These are s-only isotopes. The about 30 s- and about 40 r-only isotopes provide a means to distinguish between the two processes.

2 The n_TOF facility

The n_TOF facility, based on an idea by Rubbia at al. [7], locate at CERN Geneva Switzerland became fully operational in May 2002, when the scientific program has started. A detailed description can be found in ref [8]. Neutrons are produced by spallation reaction induced by a pulsed, 6 ns wide, 20 GeV/c proton beam with up to $7x10^{12}$ proton per pulse, impinging on a 80x80x60 cm^3 lead target. A 5.8 cm water slab surrounds the lead target acting as a coolant and as moderator of the initial fast neutron spectrum. An isolethargic neutron flux distribution is produced over a wide range of energy (1 eV – 250 MeV).

Neutrons emerging from the target propagate in the vacuum pipe inside the time-of-flight tunnel 200 m long. Two collimators are present along the flight path, one of the diameter of 13,5 cm placed at 135 m from the lead target and one at 180 m with a diameter of 2 cm for the capture measurements. This collimation results in a Gaussian-shaped beam profile [9]. A 1.5 T sweeping magnet placed at 40 m upstream of the experimental area is used to deflect outside the beam charged particles travelling along the vacuum pipe. For an efficient background suppression, several concrete and iron walls are placed along the time-of-flight tunnel.

The measuring station is located inside the tunnel, centered at 187.5 m from the spallation target.

The neutron beam is monitored up to 1 MeV by a low-mass system, based on thin mylar foil with ^{6}Li deposit places in the beam, surrounded by an array of silicon detectors place outside the beam. The detection by the silicon detectors of the triton and α s produced in the ^{6}Li(n,α) reaction gives a direct measure of the neutron flux. The small amount of material in the beam ensures a negligible level of scattered neutrons. The scattering chamber is made in carbon fibre to minimize the neutron-induced γ background.

Measurements of neutron capture cross-sections in the first stage of the project were performed with specifically made C_6D_6 detectors, and in the second stage of the measurements a 4π calorimeter made of 40 BaF_2 crystal has been used.

The data acquisition system is based on flash ADCs with sampling rate up to 1 GHz for recording the detector signals during nearly 20 ms off-line analysis. This generate a high data rate but ensures an almost zero dead-time.

In the first phase of the n_TOF project, neutron capture measurements were carried with an array of C_6D_6 liquid scintillator cells. These detectors have the advantage of being the less sensitive to scattered neutron. Specifically designed C_6D_6 where used at n_TOF, in order to reduce the neutron sensitivity all the material that could produce a neutron capture in the detector were removed or substituted, all the aluminum part were substituted with carbon fibre [10] and also the support material was minimized, allowing to perform measurement of isotopes with a large scattering to capture ratio.

Due to the small solid angle coverage and the low intrinsic efficiency the C_6D_6 detectors, which result in an overall efficiency of ~10%, only one γ-ray per event is detected from the de-excitation cascade following neutron capture. For an accurate cross-section determination, the efficiency of the set-up has to be made independent on the details of the de-excitation cascade, in particular of the γ-ray multiplicity.

To this end the pulse height weighting function (PHWF) has been used. It consists in suitably modifying by software the detectors response so that the efficiency ε_γ is proportional to the photon energy E_γ. Under these conditions the efficiency for detecting a cascade becomes proportional to the known cascade energy Ec and independent of the actual cascade path.

In the second phase of n_TOF project the neutron capture measurements have been performed with Total Absorption Calorimeter (TAC). The design of the n_TOF TAC is based o 42-fold segmentation consisting of 15 cm thick BaF_2 crystal in the form of truncated pyramids. Each of the 12 pentagonal and 30 hexagonal crystals extends the same solid angle with respect to the sample centre.

On average the crystals exhibit an average energy resolution of 14% at 662 keV and an excellent time resolution of about 500 ps.

Due to the low cross-section of most the samples of Astrophysics interest measured at n_TOF, the C_6D_6 were preferred for these measurements since the background due to the in-beam γ for those detectors is lower.

3 Experimental campaign

The Astrophysics experimental campaign was focus on neutron magic nuclei, which act as bottle neck for the flow of s-process, nuclei with $A < 120$, branching points isotopes and isotopes of special interest as the Os important for nuclear cosmochronology.

In the following the description and results of the measurements.

3.1 ^{151}Sm(n,γ) cross section measurements

The ^{151}Sm is a branching point in the s-process path, in particular, this branching is sensitive to the temperature at which the s-process is taking place. The accurate determination of the neutron capture cross-section of this isotope can thus provide crucial information on the thermodynamics condition of the AGB stars.

The measurement had been performed with the C_6D_6 liquid scintillator. The result obtained at n_TOF is $<\sigma(n,\gamma)> = 3100 \pm 160$ mb, a value much larger than previous estimated, all based on model calculation, which ranged from 1500 and 2800 mb [11].

The firm estimate of the capture rate for the first time base on experimental value allowed reaching two important conclusions with respect to the s-process nucleosynthesis in this mass region: i) the classical model, based on the phenomenological study of the s-process fails to produce consistent result of the branching at ^{151}Sm and ^{147}Pm, ii) the p-process contribution to the production of ^{152}Gd can amount up 30% of the solar-system observed abundance [11]

3.2 ^{90,01,92,93,94,96}Zr(n,γ) measurements

Zr is a typical s-process element belonging to the first s-process peak of solar abundance distribution. Predictions of the production of the various Zr isotopes are critical for s-process modelling. Several of them are close to the magic number of neutron N =50, with ^{90}Zr having exactly N=50. Hence, production of ^{90,91,92,93,94}Zr is sensitive to the overall neutron flux, which is mostly defined by the ^{13}C neutron source. The abundance of the remaining stable isotope, ^{96}Zr, is determined by the activation of the branching point at the unstable ^{95}Zr. Hence, its production is sensitive to the neutron density, which is mostly defined by the ^{22}Ne neutron source. Furthermore, most of the abundance of the element Nb is due to the radiogenic decay of the long living ^{93}Zr (1.6 My).

The capture cross sections of the ^{91,92,93,94,96}Zr in term of resonance parameter were measured in a wide neutron energy range. The results [12,13,14,15,16] show sizeable differences with respect to previous experimental data and allow extracting the related nuclear quantities with improved accuracy.

3.3 ^{204,206,207}Pb and ^{209}Bi(n,γ) measurements

The Pb isotopes and the ^{209}Bi have a special role in the nucleosynthesis, these isotopes represent the termination point of s-process nucleosynthesis, this point is reached since the α-recycling of Po and heavier Bi isotopes is always faster than further neutron captures. It is important to know the cross section information for the Pb and Bi isotopes with very high accuracy in order to determine more exactly the amounts and ratios of these isotopes being produced.

Capture widths and radioactive kernels were determinate in a large range of energy for all isotopes. From these results the MACS have been derived and in many cases large discrepancy were found with values of the previous experiment, in figure 2 is reported the comparison between the ^{204}Pb MACS calculated with n_TOF and the values reported by Bao [17],

For all isotopes the systematic uncertainties could be improved by a factor two, this allowed to have a firm calculation of the abundances of the s-process component and to constrain the estimation of the r-process component, the results are reported in [18][19][20][21].

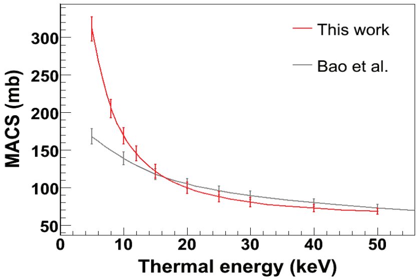

Fig. 2 Comparison between the ^{204}Pb MACS calculated with n_TOF data and Bao et al.

3.4 ^{186,187,188}Os measurements

The time duration of the nucleosynthesis of the heavy elements produced by neutron capture processes can be used to set limits on the age of the universe [22]. Among several cosmic clock based on the abundances of long-lived radioactive isotopes, the ^{187}Os/^{187}Re is one of the most interesting.

The clock is based on the extremely long half-life of ^{187}Re($\tau_{1/2}$ = 43.3Gyr), decaying to ^{187}Os, and on the fact that ^{186}Os and ^{187}Os are shielded against direct r-process production. Thanks to the well established s-process abundances of the ^{186}Os and ^{187}Os, the age of the Universe can be inferred, in the the Re/Os clock, by the enhancement in the abundance of ^{187}Os due to $^{187}\text{Re} \rightarrow ^{187}\text{Os}$ decay.

The neutron capture cross sections of ^{186,187,188}Os have been measured at the CERN n_TOF facility with improved accuracy and over a wide energy range of neutron energies from 1 eV to 1 MeV. In Fig. 3 a comparison between the n_TOF result and the previous data is shown. Based on the n_TOF data, Maxwellian averaged cross sections have been obtained with uncertainties between 3 and 4%. These results have been complemented by a detailed resonance analysis. Average level spacing, radiative widths, and neutron strength functions have been deduced by statistical analysis to establish a consistent set of input data for detailed cross section calculations with the Hauser-Feshbach statistical model. Based on these calculations stellar enhancement factors were obtained to correct the Maxwellian averaged cross sections determined from experimental (n,γ) data for the effect of thermally excited states in the hot, dense photon bath at the *s*-process site. The corresponding stellar (n,γ) cross sections have been used to separate the radiogenic part of the ^{187}Os abundance from its *s*-process component and to define the mother/daughter ratio ^{187}Re/^{187}Os. With a schematic model that assumes an exponentially decreasing production rate for ^{187}Re, an age of the Universe of 15.3+-0.8+-2 Gyr was obtained from the Re/Os cosmo-cronometer, with an accuracy, mostly related to the remaining nuclear physics uncertainties, of less than 1 Gyr. More details can be found in [23,24,25]

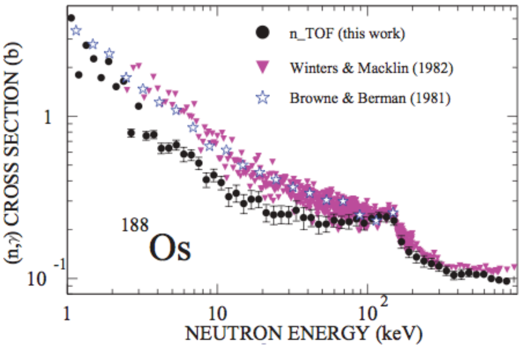

Fig. 3 Comparison between the present results and the previous data [24]

4 Conclusion

Neutron capture cross sections of astrophysical interest have been measured at the CERN n_TOF facility. The major motivation of these measurements was to reduce the uncertainties on nuclear data to a few percent, as required to improve the stellar s-process model.

In 2010 the facility was upgraded, the spallation target and moderator were substitued, the upgrade improved the n_TOF apparatus resulting in a significantly reduction of the uncertainty in the measured cross-sections, with a valuable impact on studies of s-process nucleosynthesis. New measurements on neutron-magic nuclei and, especially, on branching-point radioactive isotopes, have been done at n_TOF, called n_TOF phase II, while a much higher neutron flux in a second experimental area at 20 m from the spallation target should be available in 2014. The new experimental area will open the way to measurements of relatively short-lived isotopes, produced at ISOLDE, involved in r-process nucleosynthesis.

References

[1] R. A. Alpher, H. A. Bethe, G. Gamow, Phys. Rev. 73 (1948) 803.

[2] E. M. Burbidge, G. R. Burbidge, W. A. Fowler, F. Hoyle, Synthesis of the elements in stars, Rev. Mod. Phys. 29, (1957) 547.

[3] G. Wallerstein, et al., Synthesis of the elements in stars: forty years of progress, Rev. Mod. Phys. 62(1999)395.

[4] M. Arnould, K. Takahash, Nuclear astrophysics, Rep. Prog. Phys. 62(1999)395.

[5] A. G. W. Cameron, Pub. Astr. Soc. Pacific 69 (1957) 201.

[6] P.W. Merrill, Science 115(1952)484.

[7] C. Rubbia et al., Tech. Rep. CERN/LHC/98-02 CERN(1998)

[8] U. Abbondanno et al., Tech. Rep. CERN/SL/2002-053 ECT(2003)

[9] S. J. Pancin et al., Nucl. Instr. Meth. A 524 (2004)102.

[10] R. Plag et al., Nucl. Instr. Meth. A 496 (2003)425.

[11] *U. Abbondanno et al.,* Phys. Rev. Letters 93 (2004)161103.

[12] G. Tagliente et al., Phys. Rev. C 77 (2008) 035802.

[13] G. Tagliente et al., Phys. Rev. C 78 (2008) 045804.

[14] G. Tagliente et al., Phys. Rev. C 81 (2010) 055801.

[15] G. Tagliente et al., Phys. Rev. C 84(2011) 015801

[16] G. Tagliente et al., Phys. Rev. C 84(2011) 055802

[17] Z.Y. Bao et al., At. Data Nucl. Data Tables 76 (2000).

[18] C. Domingo-Pardo et al., Phys Rev. C75 (2007) 15806.

[19] C. Domingo-Pardo et al., Phys Rev. C74 (2006) 55802.

[20] C. Domingo-Pardo et al., Phys Rev. C74 (2006) 25807.

[21] C. Domingo-Pardo et al., Phys Rev. C76 (2007) 45805.

[22] D. D. Clayton et al., *Cosmoradiogenic chronologies of nucleosynthesis* // Ap. J. – 1964 – Vol. 139. – P. 637.

[23] M. Mosconi et al., Neutron physics of the Re/Os clock. I. Measurement of the (n,γ) cross sections of ^{186,187,188}Os at the CERN n TOF facility// Phys. Rev. C 82 (2010) 015802.

[24] M. Mosconi et al., Neutron physics of the Re/Os clock. II. The (n,n') cross section of 187Os at 30 keV neutron energy // Phys. Rev. C 82 (2010) 015803.

[25] K. Fujii et al., Neutron physics of the Re/Os clock. III. Resonance analyses and stellar (n,γ) cross sections of ^{186,187,188}Os // Phys. Rev. C 82 (2010) 015804.